# Supplementary material 5:

# Effect of plastic deformation of austenite

## a) Nucleation of martensite at intersection of glide planes.

Strain-induced nucleation of martensite was clearly shown to involve shear systems of austenite (Olson & Cohen, 1972). The fact that martensite tends to form at the intersection of two shear bands of austenite can be explained with the one-step theory. Such a situation can be illustrated by using the TEM images of Shimizu and Nishiyama (1972) reported in Fig. S5_1. This image is also discussed in Nishiyama's book (1978). On the M2 part, the martensite nucleates at the intersection of two $\{111\}_\gamma$ glide plane (only faint trace of the right one is visible). The HP plane of the new formed martensite M2 is $\{225\}_\gamma$ and Nishiyama noticed that from all the equivalent $\{225\}_\gamma$ planes only those at 25° from the $\{111\}_\gamma$ glide plane can appear. He added "*this fact must be taken into account in the nucleation theories*". By keeping the reference frame used in Fig. 3, that fact can be understood as follows. Let assume that the TEM image was acquired with an electron beam close to the neutral line $[110]_\gamma$ // $[111]_\alpha$, the glide plane can be indexed as $(1\bar{1}1)_\gamma$ and the HP as $(2\bar{2}5)_\gamma$, which should also be a $\{112\}_\alpha$ plane for the martensite in Pitsch OR (but no indication is given by Nishiyama on that point). The $(2\bar{2}5)_\gamma$ and $(1\bar{1}1)_\gamma$ planes make an angle of 25.24°. It can also be noticed that the $(1\bar{1}1)_\gamma$ glide plane is transformed into a stacking fault beyond the intersection point. Such an observation can be explained by considering the Lomer-Cottrell locks. They were introduced in section 4.1 without taking into account the dissociation of dislocations into Shockley partials for sake of simplicity, but actually, the ½$[0\bar{1}1]_\gamma$ dislocation lying on $(\bar{1}11)_\gamma$ plane and the ½$[10\bar{1}]_\gamma$ dislocation lying on the $(1\bar{1}1)_\gamma$ plane dissociate during combination; the former is split into 1/6 $[\bar{1}\bar{2}1]_\gamma$ and 1/6 $[1\bar{1}2]_\gamma$, and the latter into 1/6 $[21\bar{1}]_\gamma$ and 1/6 $[1\bar{1}\bar{2}]_\gamma$. The first members of each pair attract each other and combine according to

$$1/6\ [\bar{1}\bar{2}1]_\gamma + 1/6\ [21\bar{1}]_\gamma \rightarrow 1/6\ [1\bar{1}0]_\gamma \qquad (1)$$

The resulting edge dislocations of Burgers vector 1/6 $[1\bar{1}0]_\gamma$ and line x = $[110]_\gamma$ are sessile. They pile-up in the $(001)_\gamma$ plane and form the edge disclination. Even if not reported in literature to our knowledge, one can imagine that the residual Shockley partials 1/6 $[1\bar{1}2]_\gamma$ and 1/6 $[1\bar{1}\bar{2}]_\gamma$ continue to glide in their respective $(\bar{1}11)_\gamma$ and $(1\bar{1}1)_\gamma$ planes, transforming their glide plane into stacking faults, as observed in Fig. S5_1a (at least for the visible glide plane). A schematic drawing with lattice and atomic positions has been added in Fig. S5_1b, without taking into account the atom reorganization at the $\gamma/\alpha$ interface. Dissociations of perfect dislocations into Shockley partials associated to $(225)_\gamma$ martensite and stacking fault have been observed by TEM in Fe-Cr-C alloys (Sandvik & Wayman, 1983).

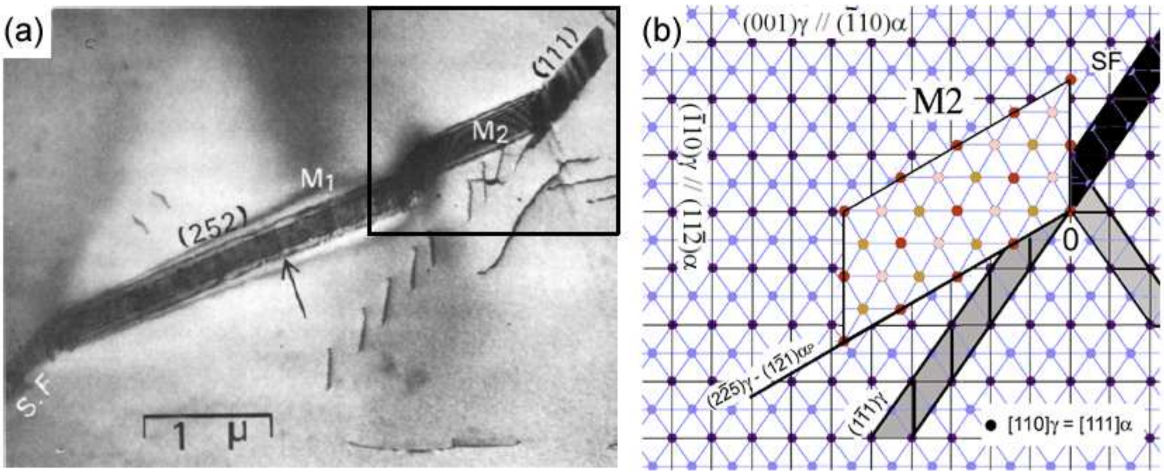


*Fig. S5_1. Formation of a martensite lath with $(2\bar{2}5)_\gamma$ habit plane. (a) TEM image from Shimizu & Nishiyama (1972) showing at the up right corner the formation of a martensite $M_2$ at the junction of two $\{111\}_\gamma$ austenite glide planes. (b) Schematic presentation with the lattices of the phases and the indices used in the text. The $(1\bar{1}1)_\gamma$ glide plane is in grey with dislocations represented by the black vertical lines. This glide plane is transformed into the stacking fault (SF) indicated by the black band.*

## b) Variant selection at intersection of glide planes.

Very recently, Gong *et al.* (2013) reported a strong variant selection of bainite transformation by ausforming. They showed that the bainitic laths are in NW OR and are grouped by packets of four variants. One of their experimental results is reported in Fig. S5_2a and b. By using the software GenOVa (Cayron, 2007a), one can show that these variants form a packet generated by the same Pitsch distortion along a unique $<110>_\gamma$ neutral line, as predicted by the one-step theory. The variants can indeed be indexed as variants NW1+NW2+NW4+NW5 according to the numbers given in Fig.9. All these variants share a common direction $<11,11,9>_\alpha$ parallel to the $<110>_\gamma$ neutral line as illustrated in Fig. S5_2d. This direction corresponds to the initial $<111>_\alpha$ // $<110>_\gamma$ direction of the Pitsch twinned nuclei P1-P2.

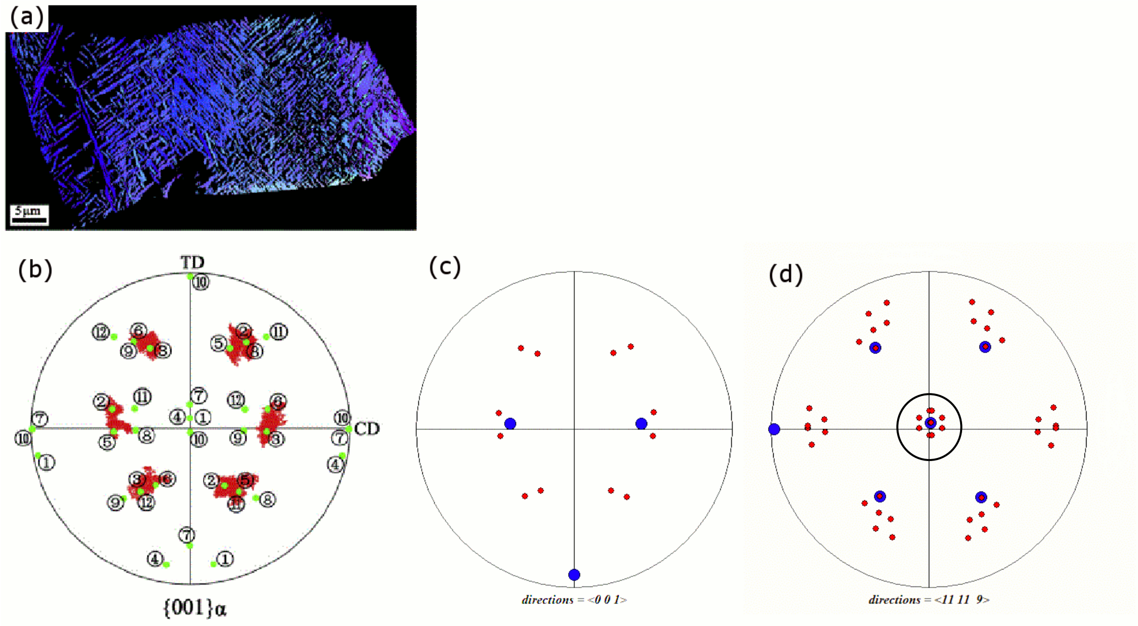


*Fig. S5_2. Variant selection in ausformed bainite (a) EBSD map and (b) <100>$_\alpha$ pole figure of the bainitic variants, from Gong et al. (2013). (c) Simulation with the variants NW1+NW2+NW4+NW5 of Fig.9. (c) pole figure of the <100>$_\alpha$ (in red) and <100>$_\gamma$ (in blue), and (d) pole figure of the <11,11,9>$_\alpha$ (in red) and <110>$_\gamma$ (in blue). The four variants share a common <11,11,9>$_\alpha$ //<110>$_\gamma$ direction (marked by the circle).*